MOLECULAR AND CELLULAR BIOLOGY, Dec. 2002, p. 8226–8240 Vol. 22, No. 23
0270-7306/02/$04.00+0 DOI: 10.1128/MCB.22.23.8226–8240.2002

PEX11α Is Required for Peroxisome Proliferation in Response to 4-Phenylbutyrate but Is Dispensable for Peroxisome Proliferator-Activated Receptor Alpha-Mediated Peroxisome Proliferation

Xiaoling Li,[1] Eveline Baumgart,[1] Gao-Xiang Dong,[2] James C. Morrell,[1] Gerardo Jimenez-Sanchez,[3] David Valle,[3] Kirby D. Smith,[2] and Stephen J. Gould[1]*

Department of Biological Chemistry,[1] Kennedy Krieger Institute and Department of Neurology,[2] and Howard Hughes Medical Institute and Departments of Pediatrics and of Molecular Biology and Genetics,[3] The Johns Hopkins University School of Medicine, Baltimore, Maryland 21205

Received 17 January 2002/Returned for modification 18 March 2002/Accepted 26 July 2002

The PEX11 peroxisomal membrane proteins promote peroxisome division in multiple eukaryotes. As part of our effort to understand the molecular and physiological functions of PEX11 proteins, we disrupted the mouse *PEX11*α gene. Overexpression of *PEX11*α is sufficient to promote peroxisome division, and a class of chemicals known as peroxisome proliferating agents (PPAs) induce the expression of *PEX11*α and promote peroxisome division. These observations led to the hypothesis that PPAs induce peroxisome abundance by enhancing *PEX11*α expression. The phenotypes of *PEX11*$\alpha^{-/-}$ mice indicate that this hypothesis remains valid for a novel class of PPAs that act independently of peroxisome proliferator-activated receptor alpha (PPARα) but is not valid for the classical PPAs that act as activators of PPARα. Furthermore, we find that *PEX11*$\alpha^{-/-}$ mice have normal peroxisome abundance and that cells lacking both *PEX11*α and *PEX11*β, a second mammalian *PEX11* gene, have no greater defect in peroxisome abundance than do cells lacking only *PEX11*β. Finally, we report the identification of a third mammalian *PEX11* gene, *PEX11*γ, and show that it too encodes a peroxisomal protein.

Peroxisomes are single membrane-bound organelles that participate in a wide variety of metabolic pathways, such as β-oxidization of very-long-chain fatty acids (VLCFAs), α- and β-oxidization of long branched-chain fatty acids, biosynthesis of plasmalogens, and H_2O_2 metabolism (45, 47, 48). These peroxisomal activities are crucial to human development, as evident from the many diseases that result from defects in peroxisomal enzymes or in peroxisome biogenesis, most of which are lethal (12, 30, 47, 48). Not surprisingly, the abundance of peroxisomes and peroxisomal enzymes is regulated in response to metabolic and environmental variables in a variety of species (42).

The abundance of peroxisomes reflects the rates of peroxisome destruction and peroxisome synthesis. Peroxisome destruction involves a specialized version of autophagy and many of the APG/CVT genes that are involved in cytoplasm-to-vacuole transport (20). Although regulated peroxisome destruction has been described for methylotrophic yeast (4), there is as yet no evidence for regulated peroxisome destruction in other yeasts or in mammals. However, there is strong evidence for regulatory pathways that couple environmental, dietary, or hormonal signals to an increased rate of peroxisome synthesis in both lower and higher eukaryotes (7, 32, 43).

The best-characterized examples of regulated peroxisome synthesis are the increases in peroxisome division that occur in yeasts in response to fatty acids (9, 27) and in mammals, notably rodents, in response to peroxisome proliferating agents (PPAs) (32). In yeast, fatty acids and/or fatty acid metabolism induces a significant increase in peroxisome abundance as well as in the expression of many genes encoding peroxisomal enzymes and peroxisome biogenesis factors (also known as peroxins). The transcriptional effects are mediated by the PIP2/OAF1 heterodimeric transcription factor (18, 34), but the molecular mechanism linking the increased expression of these enzymes, biogenesis factors (peroxins), and metabolic activities to increases in peroxisome formation remains obscure.

It is clear that peroxisomal metabolic activities can have a profound effect on peroxisome abundance (7, 43), but it is also clear that overexpression of one peroxin, PEX11, can induce peroxisome abundance in the absence of extracellular stimuli or peroxisome metabolism (23, 38). Cells lacking PEX11 display the normal transcriptional response to fatty acids but are unable to induce peroxisome synthesis (9, 27). Conversely, overexpression of PEX11 leads to an elevated rate of peroxisome formation (9, 27), even in the absence of exogenous fatty acids or peroxisomal fatty acid metabolism (23). More recently, Hoepfner et al. (13) identified the dynamin-like GTPase VPS1 as required for peroxisome division. Although overexpression of VPS1 does not induce peroxisome division, cells lacking VPS1 have even fewer peroxisomes than do *pex11* mutants (13; X. Li and S. J. Gould, submitted for publication).

Similar observations have been derived from mammalian cell studies. In fact, the first observations of peroxisome pro-

* Corresponding author. Mailing address: Department of Biological Chemistry, The Johns Hopkins University School of Medicine, 725 North Wolfe S., Baltimore, MD 21205. Phone: (410) 955-3424. Fax: (410) 955-0215. E-mail: sgould@jhmi.edu.

liferation were obtained from studies of fibrate drugs in rodents (5, 32). Exposure of rats and mice to these hypolipidemic drugs caused peroxisome abundance to rise dramatically, particularly in the liver, and also increased the expression of many peroxisomal enzymes involved in fatty acid oxidation. These drugs bind to the peroxisome proliferator-activated receptor alpha (PPARα) and stimulate the activity of a heterodimeric transcription factor composed of PPARα and the 9-*cis*-retinoic acid receptor (RxR). The activation of PPARα/RxR leads to increased expression of numerous lipid-metabolizing enzymes, including those of the peroxisomal fatty acid β-oxidation pathway (32), and increased expression of PEX11α (31, 38). Unlike yeasts, mammals have multiple *PEX11* genes and the expression of either *PEX11*α or *PEX11*β is sufficient to induce peroxisome division in cultured cells. Peroxisome division in mammals also requires a large dynamin-like GTPase, the dynamin-like protein 1 (DLP1) (Li and Gould, submitted), and is influenced by the metabolic state of the peroxisome (7, 43). Thus, the regulation of peroxisome division follows similar themes in both yeast and mammalian cells, though there appear to be additional layers of complexity to the mammalian system.

Studies of PEX11 are concerned not only with its role in peroxisome formation but also its potential metabolic and physiological roles. The yeast *pex11* mutant and the *PEX11*β-deficient mouse are both defective in certain aspects of peroxisome metabolism (22, 43). Furthermore, *PEX11*β deficiency in mice can cause intrauterine growth defects, neonatal lethality, hypotonia, neuronal migration defects, and enhanced neuronal apoptosis (22). These phenotypes are extremely similar to those of Zellweger syndrome mice and Zellweger syndrome patients, though they lack the peroxisomal protein import defects and strong metabolic defects of Zellweger syndrome and its mouse models (12). As a result, it may be that the pathophysiology of Zellweger syndrome is caused by a more subtle metabolic defect than previously assumed and, hence, may be more amenable to therapeutic intervention once the causative metabolic defect is identified. Whether the pathologically relevant metabolic defect in *PEX11*$\beta^{-/-}$ animals is due to a direct role for PEX11β or is an indirect consequence of reduced peroxisome abundance remains to be determined.

In an effort to improve our understanding of PEX11 function in general, and the physiological roles of PEX11α in particular, we generated a mouse strain carrying a disruption of the *PEX11*α gene. Unlike *PEX11*β-deficient mice, mice lacking *PEX11*α are externally indistinguishable from their wild-type (WT) and heterozygous littermates and follow a seemingly normal developmental pattern. Furthermore, they have no detectable defect in constitutive peroxisome division and, more surprisingly, display a normal peroxisome proliferation response when exposed to PPARα-activating drugs. However, cells lacking PEX11 are defective in peroxisome proliferation induced by 4-phenylbutyrate (4-PBA), an atypical PPA that acts independently of PPARα. We also report the phenotypes of mice lacking both the *PEX11*α and *PEX11*β genes and describe a third *PEX11* gene, *PEX11*γ.

MATERIALS AND METHODS

Generating mutant mice. A genomic DNA clone of the mouse *PEX11*α gene was identified by screening a genomic DNA BAC library of 129J/Sv mice with the full-length mouse *PEX11*α cDNA (38). Three continuous *Nhe*I-*Nhe*I fragments from this BAC clone, spanning an 18-kb genomic region containing the *PEX11*α gene, were subcloned into the pLITMUS38 vector (New England BioLabs, Beverly, Mass.) and sequenced. The deduced genomic structure of the *PEX11*α gene is shown in Fig. 1A. The targeting vector (Fig. 1A), designed to disrupt the last two exons of the *PEX11*α gene, was generated by flanking the 5′ and 3′ regions of the pgk-Neo^R cassette in the pGT-N 28 vector (New England BioLabs) with a 3.6-kb *Sca*I-*Aat*II fragment (5′ untranslated region and exon 1) and a 3.0-kb *Nhe*I-*Pvu*II fragment (3′ untranslated region) of the *PEX11*α gene, respectively. The resulting targeting vector (200 μg) was linearized with *Swa*I and electroporated into 6.5×10^6 R1 embryonic stem (ES) cells as previously described (49). Transfected cells were plated onto Neo^R, mitomycin C-inactivated primary embryonic fibroblasts. After 24 h of growth, the medium was supplemented with 200 μg of G418/ml, and the cells were grown for an additional 8 to 10 days in selective medium. G418-resistant clones were examined by Southern hybridization analysis of *Nhe*I- or *Eco*RI-digested genomic DNA, by using two flanking probes (probes A and B, Fig. 1B). Two independently generated *PEX11*$\alpha^{+/-}$ ES cell clones were identified and injected into blastocysts of C57BL/6 host mice (Jackson Laboratory, Bar Harbor, Maine). Chimeric males derived from both *PEX11*$\alpha^{+/-}$ ES cell lines were intercrossed with C57BL/6 mice. Agouti offspring were tested for the presence of the mutant *PEX11*α allele by Southern blotting (37). Heterozygous F_1 mice were either intercrossed to produce homozygous *PEX11*$\alpha^{-/-}$ animals or backcrossed with C57BL/6 mice five times prior to generating *PEX11*$\alpha^{-/-}$ animals. Genotypes of mice from generation F_2 and beyond were determined by PCR with the following primers: primer 10, 5′-AATCAGGGACCTGTGCAACCTG-3′; primer 11, 5′-AGTACA GCGTGGCTAATGAAGAGAC-3′; and Neo primer, 5′-ATATTGCTGAAGA GCTTGGCGGC-3′. The WT allele was amplified by primer 10 and primer 11 to yield a 556-bp product, while the targeted allele was amplified by primer 10 and the Neo primer to yield a 907-bp product (Fig. 1C). An 0.1-μg amount of genomic DNA was used in a 25-μl reaction mixture.

The generation of doubly homozygous *PEX11*$\alpha^{-/-}$/*PEX11*$\beta^{-/-}$ animals was accomplished both by crossing doubly heterozygous *PEX11*$\alpha^{+/-}$/*PEX11*$\beta^{+/-}$ animals and by crossing *PEX11*$\alpha^{-/-}$/*PEX11*$\beta^{+/-}$ animals. Typing the *PEX11*β locus was accomplished as described previously (22).

Northern analysis. Total RNA was isolated from mouse livers by using the Purescript RNA isolation kit (Gentra Systems, Minneapolis, Minn.). RNA (10 μg/lane) was separated on formaldehyde-agarose gels (1.5%), transferred to GeneScreen Plus membranes (NEN Life Science Products, Boston, Mass.), and hybridized according to standard procedures (37). The expression patterns of *PEX11*α and *PEX11*γ were analyzed by probing a mouse multitissue Northern blot [2 μg of poly(A)$^+$ mRNA/lane; Clontech, Palo Alto, Calif.] with the full-length mouse *PEX11*α or *PEX11*γ cDNA. To study the effect of PPAs on mice, 6- to 8-week-old control and *PEX11*α-deficient male mice were fed with either standard chow or chow supplemented with 0.0125% ciprofibrate (Sigma, St. Louis, Mo.) for 2 or 5 weeks as indicated, and then total liver RNA was isolated and analyzed as described above.

Immunoblotting. The expression of PEX11α protein in control and *PEX11*$\alpha^{-/-}$ mouse livers was analyzed by extracting total protein from liver, separating the proteins by sodium dodecyl sulfate-polyacrylamide gel electrophoresis, transferring the proteins to polyvinylidene difluoride membranes, and probing them with rabbit antibodies generated against the C-terminal 12 amino acids of the mouse PEX11α protein. These antibodies were generated by coupling the peptide NH_2-TVVYPQLKLKAR-COOH to keyhole limpet hemocyanin (Pierce, Rockford, Ill.) and injecting it into four rabbits, one of which generated a recognizable immune response. Proteins were extracted from livers of mice fed a normal chow diet as well as from animals fed a normal chow diet that was supplemented with 0.0125% ciprofibrate for 2 weeks.

Mouse fibroblasts, immunofluorescence microscopy, and transfections. Mouse embryonic fibroblasts (MEFs) were isolated from E14.5 embryos as described elsewhere (14). For indirect immunofluorescence, cells were fixed for 20 min in 3% formaldehyde in Dulbecco's phosphate-buffered saline (PBS; pH 7.1; Life Technologies, Bethesda, Md.), permeabilized for 5 min in 1% Triton X-100–Dulbecco's PBS, and processed as described previously (7). Affinity-purified rabbit anti-human PEX14 antibody has been described previously (35), sheep anti-human catalase antibodies were obtained from The Binding Site (Birmingham, United Kingdom), anti-myc monoclonal antibodies were from the tissue culture supernatant of the hybridoma 1-9E10 (10), and labeled secondary antibodies were obtained from standard commercial sources. Transfections were done by electroporation as described previously (6).

Histology and electron microscopy. Newborn mice (P0.5) were deeply anesthetized by ether and perfused intracardially with 0.5 ml of physiological saline (150 mM NaCl, 0.05% $CaCl_2$, pH 7.4), followed by 10 ml of 4% paraformalde-

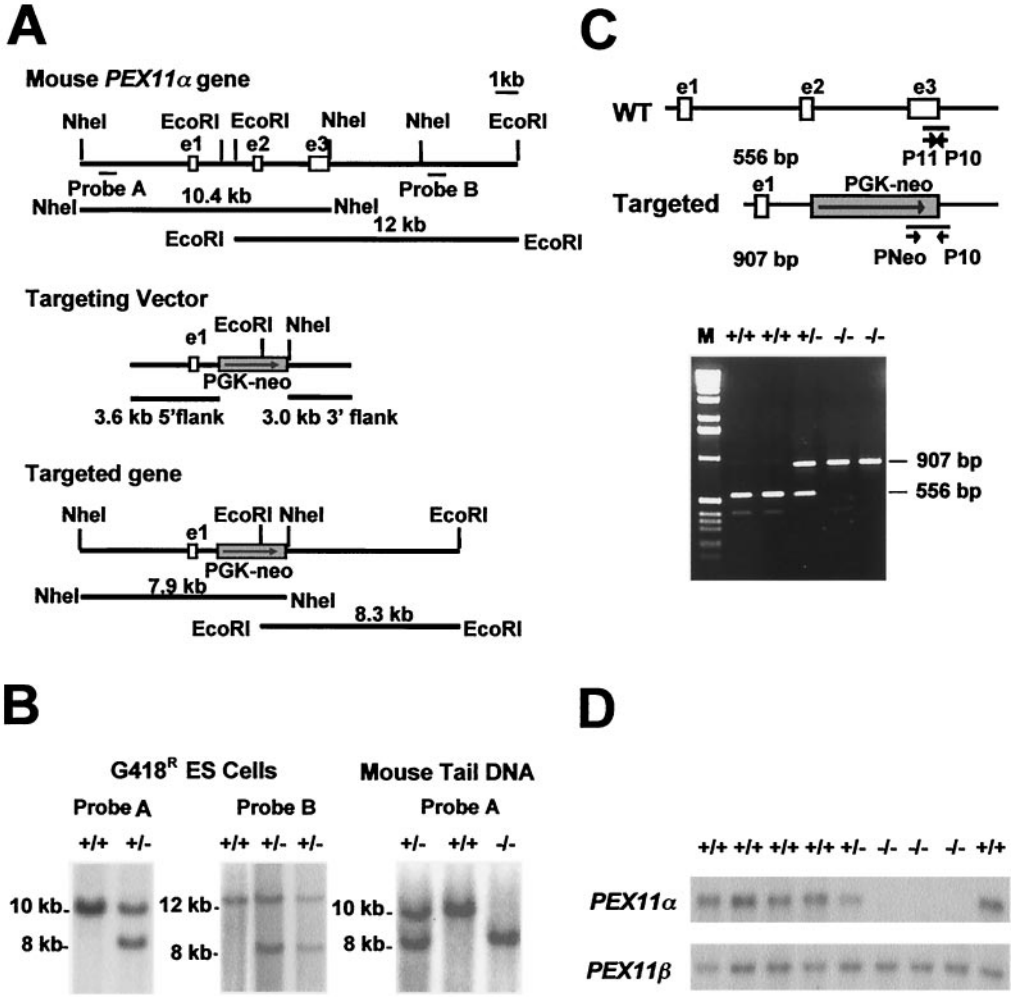

FIG. 1. Generation of *PEX11*α-deficient mice. (A) Schematic representation of the *PEX11*α WT locus (top), targeting vector (middle), and the targeted allele (bottom). Two flanking Southern blot probes, probes A and B, are indicated. (B) Southern blot analyses of the G418^R ES cell DNA with probe A (left) and probe B (middle) and the mouse tail DNA with probe A (right). Probe A detects a 10.4-kb *Nhe*I fragment in the WT allele and a 7.9-kb fragment in the targeted allele. Probe B detects a 12.0-kb *Eco*RI fragment in the WT allele and an 8.3-kb fragment in the targeted allele. (C) PCR analysis of mouse tail DNA. Positions of three primers are indicated. The WT allele product is 556 bp, and the targeted allele product is 907 bp. (D) Northern blot analysis of total liver RNA from WT (+/+), homozygous (−/−), and heterozygous (+/−) animals. The Northern blot was probed with a radioactively labeled murine *PEX11*α cDNA probe (upper panel), stripped, and probed with labeled *PEX11*β cDNA (lower panel). Note that the expression level of *PEX11*β was not elevated in the homozygous animals.

hyde in PBS, pH 7.4. The animals were then further fixed by immersion in the same fixative overnight at 4°C and paraffin embedded. Five-micrometer sagittal sections of whole mice were stained with hematoxylin and periodic acid-Schiff stain for histological analysis of body tissues. For examination of 6- to 8-week-old adult mice, animals were anesthetized with ether and perfused through the hepatic portal vein with 10 ml of physiological saline, followed by 50 ml of 4% paraformaldehyde in PBS buffer, pH 7.4. Livers were then embedded in paraffin, sectioned at 5 μm, stained with hematoxylin and periodic acid-Schiff stain, and analyzed by light microscopy.

For electron microscopy, adult mice were anesthetized with ether and perfused through the hepatic portal vein first with 10 ml of physiological saline and then with 50 ml of 4% paraformaldehyde–0.05% glutaraldehyde–2% sucrose–0.05% $CaCl_2$, in 0.1 M piperazine-*N*,*N*′-bis(2-ethanesulfonic acid) (PIPES) buffer, pH 7.4. Livers were then removed, cut into 100-μm sections, and postfixed for 15 min with 1.0% glutaraldehyde in 0.1 M PIPES buffer. Catalase cytochemistry was performed with the alkaline diaminobenzidine (DAB) medium according to the method of Fahimi (11). DAB-stained sections were postfixed with either aqueous or reduced osmium, embedded in Epon 812, and examined by electron microscopy.

Measuring peroxisome abundance. To determine peroxisome abundance in mouse fibroblasts, fluorescence images were captured with an UltraVIEW confocal imaging system (Nikon) and analyzed with IPLab software (Scanalytics, Fairfax, Va.). Peroxisomes in the widest region of the cell, in 0.5-μm-thick sections, were automatically identified as segments comprised of pixels with a limited range of intensity, and then the segments in each cell were automatically counted (peroxisomes per section). At least 100 randomly selected cells were examined for each sample. To determine the peroxisome abundance in mouse livers, Epon-embedded alkaline DAB-stained mouse livers were sectioned at 0.5 μm, analyzed under an inverted Zeiss microscope (Axiovert 135 TV; Thornwood, N.Y.), and digitally photographed. For each experimental group, 50 to 80 independent fields (5,785 μm^2 each) were photographed from four animals, and then DAB-stained peroxisomes and the empty spaces between hepatocytes were automatically measured with IPLab software. Peroxisome density was then obtained according to the following equation: $D = P \times 5{,}000/(A_{field} - A_{empty})$, where D is the peroxisome density (peroxisomes/5,000 μm^2), P is the peroxisome number in a 5,785-μm^2 field, A_{field} is the area of the photograph field (5,785 μm^2 in this study), and A_{empty} is the area of the empty spaces between hepatocytes. Ciprofibrate-treated animals were fed normal chow supplemented with 0.0125%

(wt/wt) ciprofibrate for 2 weeks, WY-14,643-treated animals were fed normal chow supplemented with 0.1% (wt/wt) WY-14,643 for 2 weeks, and diethylhexylphthalate (DEHP)-treated animals were fed normal chow supplemented with 2% (vol/wt) DEHP for 2 weeks.

4-PBA treatment of MEFs. To study the effect of 4-PBA on the peroxisome proliferation in *PEX11*α-deficient cells, control and *PEX11*$\alpha^{-/-}$ MEFs were cultured in standard medium (39) supplemented with 5 mM 4-PBA for 10 days and then fixed and processed for indirect immunofluorescence for catalase and PEX14. Cell images were then taken under a normal immunofluorescence microscope and enlarged to count the number of peroxisomes in each cell with the aid of a colony counter.

Biochemical assays. For lipid analysis in plasma and MEFs, total lipids in the plasma and fibroblasts were extracted with choroform-methanol-water, converted to their methyl esters, dissolved in hexane at a concentration of ~1 μg/μl, and separated by gas chromatography (DB-1 and SP-2560 columns) as described previously (29). Fatty acid levels were normalized as the percentage of the total amount of lipids in the extracts. Oxidation assays for the branched-chain fatty acids phytanic acid and pristanic acid were carried out in cultured embryonic fibroblasts with [2,3-^{3}H]phytanic acid or [1-^{14}C]pristanic acid as substrate (50, 53). Fatty acid β-oxidation assays were carried out with liver homogenates with [1-^{14}C]palmitic acid ($C_{16:0}$) and [1-^{14}C]lignoceric acid ($C_{24:0}$) as substrate (50). Plasmalogen synthesis activity was determined in the cultured MEFs by the double-substrate, double-isotope method (33).

Cloning the *PEX11*γ gene. To identify the human cDNA with the potential to encode a protein similar to the human PEX11α and PEX11β proteins, we scanned the completed human genome sequence with the TBLASTN algorithm (3) with the use of human PEX11β as the query. Although several regions in human chromosomes have been identified as encoding possible PEX11 homologs, only one of them (in chromosome 19) has two overlapping expressed sequence tags in the database of expression sequence tags. Iterative searches led to the identification of human and mouse cDNA clones in the I.M.A.G.E. Consortium that were likely to encode the entire open reading frame of this gene, which we designated *PEX11*γ. These cDNA clones were sequenced in their entirety (accession numbers are given below). To determine the subcellular distribution of the *PEX11*γ gene product, the open reading frames of the human and mouse cDNAs were amplified with oligonucleotides designed to append an *Asp*718 site upstream of the start codon (GGTACCATG) and a *Bam*HI site (GGATCC) in place of their stop codon. Following digestion with the restriction enzymes *Asp*718 and *Bam*HI, these fragments were cloned into pcDNA3myc (52). An N-myc-tagged expression vector, pcDNA3-myc*PEX11*γ, was also generated. The inserts in the resulting plasmids were sequenced to ensure the absence of any mutations in the open reading frame.

Nucleotide sequence accession number. The GenBank accession numbers for the sequenced cDNA clones are BE616000 for the human *PEX11*γ gene and BG176196 and AK007582 for the mouse *PEX11*γ gene.

RESULTS

Generation of *PEX11*α-deficient mice. To disrupt the *PEX11*α gene, we generated a targeting vector that replaced exons 2 and 3 of this gene with the pgk-Neo^{R} cassette (Fig. 1A). These two exons encode 227 of the 246 amino acids in the PEX11α protein. After linearization, this targeting vector was electroporated into R1 ES cells and transfected cells were selected with G418. G418-resistant ES clones were screened by Southern hybridization of *Nhe*I- or *Eco*RI-digested ES cell genomic DNA with two flanking probes (probes A and B, Fig. 1A and B). *PEX11*$\alpha^{+/-}$ ES cell clones were also examined with a probe specific for the Neo^{R} gene, which also showed the expected genetic alteration (data not shown). Two independently derived *PEX11*$\alpha^{+/-}$ ES clones were injected into blastocysts of C57BL/6 host mice, chimeric mice were obtained, and these mice were crossed with C57BL/6 mice. The heterozygous F_1 animals were either intercrossed to produce homozygous *PEX11*$\alpha^{-/-}$ animals or backcrossed with C57BL/6 mice for five generations to obtain *PEX11*$\alpha^{-/-}$ animals with a relatively homogeneous background.

PEX11$\alpha^{+/+}$, *PEX11*$\alpha^{+/-}$, and *PEX11*$\alpha^{-/-}$ animals were obtained in the expected Mendelian ratios (1:2:1) in numerous intercrosses between *PEX11*$\alpha^{+/-}$ animals. *PEX11*$\alpha^{-/-}$ animals lacked detectable *PEX11*α mRNA, as judged by Northern analysis (Fig. 1D). Mice of all genotypes were similar, with no obvious external phenotypes. There were no significant differences in body and liver weight between age-matched control and *PEX11*$\alpha^{-/-}$ animals, and no obvious abnormalities were detected in the histological analysis of liver, kidney, adrenal gland, intestine, heart, lung, brown adipose tissue, brain, and bone of *PEX11*$\alpha^{-/-}$ animals (data not shown).

PEX11α-deficient mice have normal peroxisome abundance. To determine whether loss of *PEX11*α affected peroxisome abundance in untreated cells, we examined mouse livers and cultured MEFs. Peroxisomes in mouse liver sections were detected cytochemically by DAB staining for the peroxisomal marker enzyme catalase, which generates an electron-dense precipitate over the organelle (Fig. 2). To detect peroxisomes in MEFs, the cells were fixed, permeabilized, and stained with antibodies specific for a peroxisomal integral membrane protein, PEX14, and a matrix enzyme, catalase (Fig. 2). DAB-stained liver sections and fluorescence-labeled fibroblasts were then analyzed by microscopy, and peroxisome abundance was determined by counting the number of distinct peroxisomal profiles. There was no statistically significant difference in peroxisome abundance between *PEX11*$\alpha^{-/-}$ mice and heterozygous and normal control animals in either liver or MEFs. Although the loss of *PEX11*α had no dramatic effect on peroxisome morphology (Fig. 3), we did observe a tendency of peroxisomes to cluster in the absence of *PEX11*α (Fig. 2B and 3B).

Peroxisome metabolism is unaffected by *PEX11*α deficiency. To determine whether loss of *PEX11*α might cause a defect in peroxisomal metabolic function, we examined major peroxisomal metabolic pathways, including fatty acid α-oxidation, fatty acid β-oxidation, and ether-lipid synthesis. Defects in peroxisomal fatty acid β-oxidation cause an approximately 10-fold increase in VLCFAs (C_{22} to C_{26}) in both plasma and fibroblasts due to a proportional defect in the oxidation of VLCFAs (47). They also cause a similar defect in the oxidation of a long branched-chain fatty acid, pristanic acid (19, 29, 47). *PEX11*$\alpha^{-/-}$ mice had normal levels of VLCFAs in plasma and fibroblasts (Fig. 4A). The oxidation of pristanic acid in embryonic fibroblasts was the same in *PEX11*$\alpha^{-/-}$ cells as in control cells (Fig. 4B), and the oxidation of palmitic acid ($C_{16:0}$) and lignoceric acid ($C_{24:0}$) in liver homogenates was the same in *PEX11*$\alpha^{-/-}$ mouse lysates as in control lysates (Fig. 4C). Peroxisomal fatty acid α-oxidation was also normal in *PEX11*$\alpha^{-/-}$ MEFs, as determined by measuring the rate of phytanic acid oxidation. In regard to peroxisomal ether-lipid synthesis, it is known that fibroblasts from patients defective in the peroxisomal plasmalogen synthesis pathway have 90 to 99% decreases in plasmalogen level and plasmalogen synthesis activity (29). However, cultured *PEX11*$\alpha^{-/-}$ fibroblasts had no significant defect in plasmalogen levels (Fig. 4D) or plasmalogen synthesis activity (Fig. 4E).

PEX11α is not required for PPA-mediated peroxisome proliferation. Like its rat ortholog, mouse *PEX11*α mRNA is expressed in a tissue-specific manner, with highest levels in liver (Fig. 5A). Mouse *PEX11*α expression is also induced by ciprofibrate, a potent fibrate peroxisome proliferator, and we also

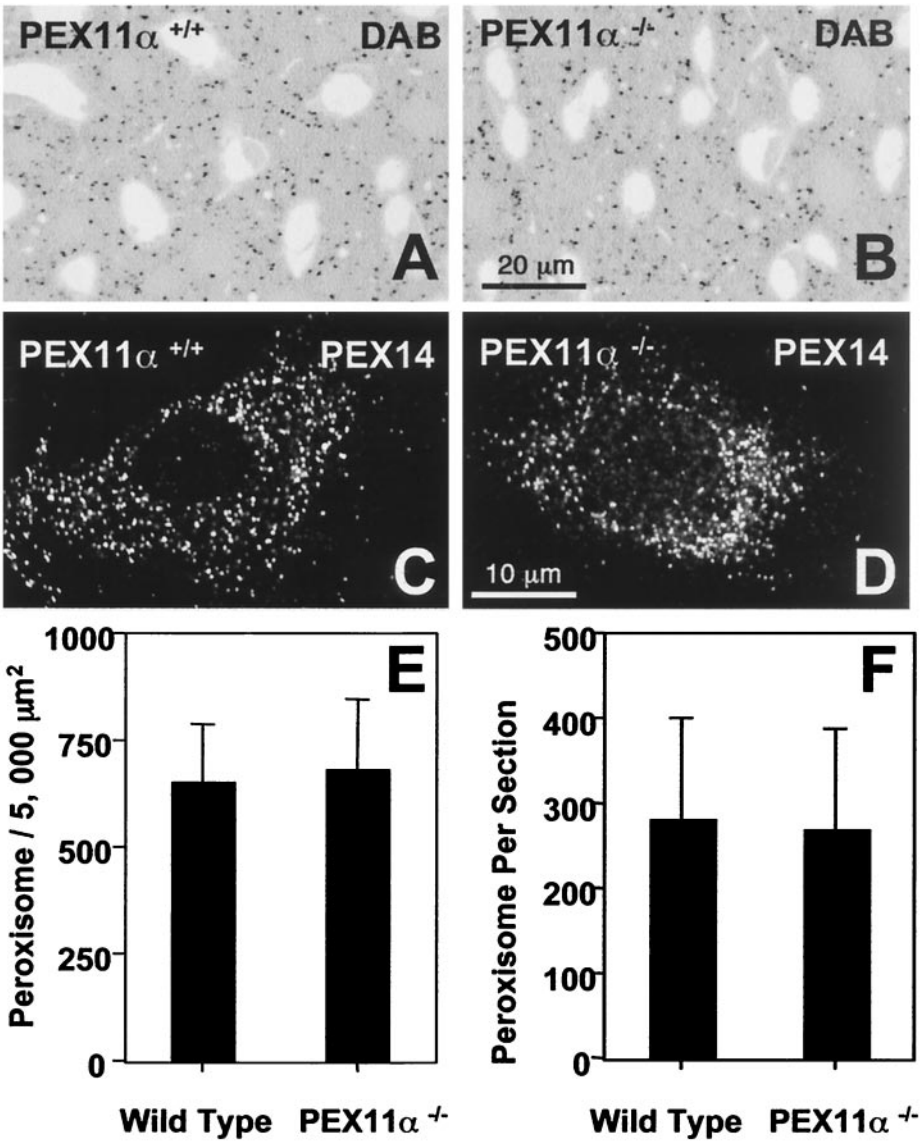

FIG. 2. Peroxisome abundance in the livers and fibroblasts of *PEX11*α-deficient mice. (A and B) Control and *PEX11*$\alpha^{-/-}$ mouse livers were fixed and stained with alkaline DAB solution for peroxisomal maker enzyme catalase. Semithin (0.5-μm) Epon-embedded sections were then analyzed under a light microscope. (C and D) MEFs from control and *PEX11*$\alpha^{-/-}$ animals were fixed, permeabilized with 1% Triton X-100, and processed for indirect immunofluorescence with antibodies to PEX14, a peroxisomal integral membrane protein. Peroxisomes present in 60 independent fields of semithin liver sections from four animals (E) and 100 randomly selected fibroblasts from three cell lines (F) were counted for each group. Results in panels E and F are presented as the average peroxisome abundances ± 1 standard deviation.

detected a significant increase in the levels of PEX11α protein following ciprofibrate treatment (Fig. 5B). As expected, we could not detect *PEX11*α mRNA or protein in *PEX11*$\alpha^{-/-}$ animals, regardless of whether the animals were fed a normal diet or the ciprofibrate-containing diet (Fig. 5B). To test whether the loss of *PEX11*α had any effect on the transcriptional response to ciprofibrate, we also examined the expression of two other PPA-inducible genes, the genes for peroxisomal 3-ketoacyl-coenzyme A thiolase (*PTL*) and cytochrome P450 4A1 (*CYP4A1*). These two genes were induced by ciprofibrate in both *PEX11*$\alpha^{-/-}$ animals and control animals. Two constitutively expressed genes, *PEX11*β and the actin gene, were unaffected by the loss of *PEX11*α and by ciprofibrate treatment (Fig. 5C).

The positive correlation between the abundance of PEX11α and peroxisome abundance indicates that PPA-mediated peroxisome proliferation might be mediated by the increased expression of PEX11α. To test this hypothesis, we measured peroxisome abundance in control and *PEX11*$\alpha^{-/-}$ animals exposed to ciprofibrate for 2 weeks. Liver sections were obtained for staining with DAB to detect peroxisomal catalase activity, and peroxisome abundance in the hepatic central vein region was determined by light microscopy. Control and *PEX11*$\alpha^{-/-}$ animals had similar peroxisome abundance before and after

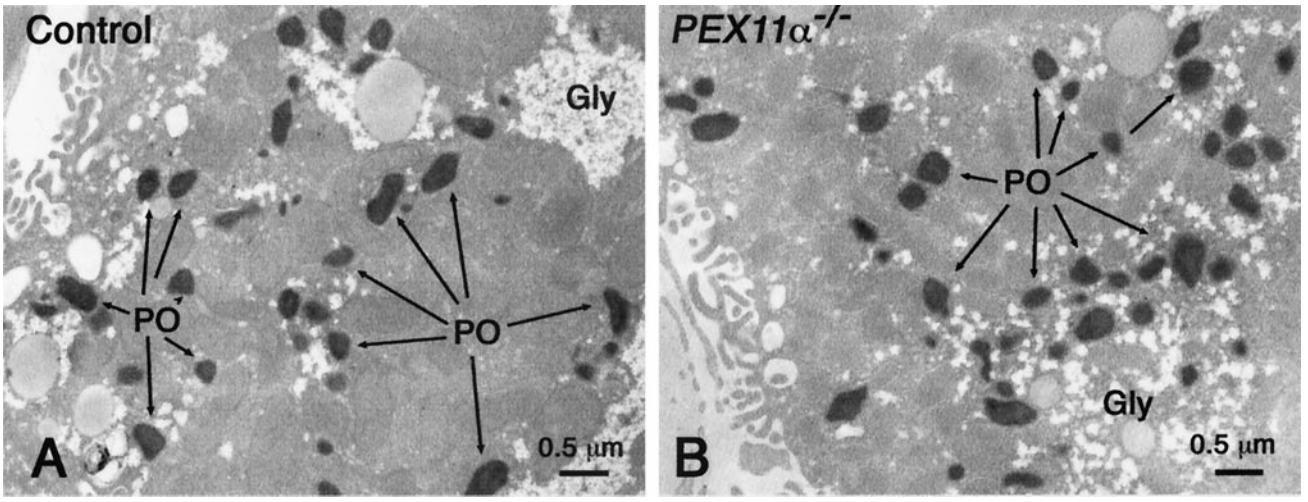

FIG. 3. Ultrastructural analysis of *PEX11*α-deficient mouse livers. DAB-stained control (A) and *PEX11*$\alpha^{-/-}$ (B) mouse liver sections were postfixed with aqueous osmium and analyzed under an electron microscope. Pictures are from the hepatic midzone. PO, peroxisome; Gly, glycogen.

exposure to ciprofibrate (Fig. 6A). In control animals, peroxisome abundance rose from 1,160 ± 240 to 2,080 ± 510 peroxisomes/5,000 μm^2 (1.6- to 4.5-fold; $P < 0.001$, Student's *t* test). In *PEX11*$\alpha^{-/-}$ animals peroxisome abundance rose from 1,140 ± 150 to 1,900 ± 540 peroxisomes/5,000 μm^2 (1.1- to 4.0-fold; $P < 0.001$, Student's *t* test). These results are reflected in representative light (Fig. 6B and C) and electron (Fig. 6D and E) microscopic images of livers from ciprofibrate-fed animals. Similar results were obtained with animals fed with ciprofibrate for 5 weeks (data not shown). The peroxisome proliferator drugs are a diverse class of compounds that includes WY-14,643 and the plasticizer DEHP in addition to ciprofibrate and many other compounds (5, 32). *PEX11*$\alpha^{-/-}$ animals exposed to these PPAs also displayed a normal peroxisome proliferation response (Fig. 6A).

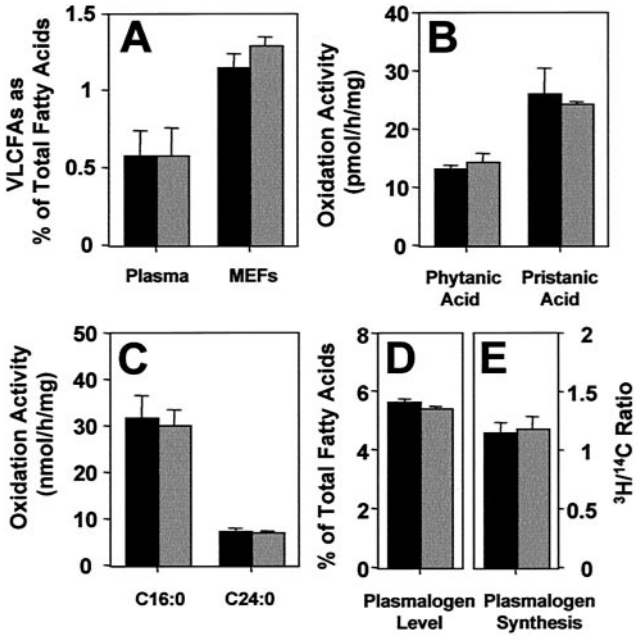

FIG. 4. *PEX11*$\alpha^{-/-}$ mice have normal peroxisome metabolic activities. In all graphs, the black bar represents the average value obtained with control samples, the gray bar represents the average value obtained with *PEX11*$\alpha^{-/-}$ mouse samples, and the brackets represent 1 standard deviation. (A) VLCFA levels in plasma and embryonic fibroblasts (MEFs) of the control and *PEX11*$\alpha^{-/-}$ mice, expressed as a percentage of total fatty acids. (B) Peroxisomal branched-chain fatty acid α- and β-oxidation activities in cultured MEFs. (C) Activities of mitochondrial ($C_{16:0}$) and peroxisomal ($C_{24:0}$) fatty acid β-oxidation in liver homogenates. (D) Plasmalogen levels in cultured MEFs, expressed as a percentage of total fatty acids. (E) Plasmalogen synthesis activities in cultured MEFs expressed as a ratio of the peroxisomal incorporation of [^{14}C]hexadecanol and the microsomal incorporation of the [^{3}H]hexadecyl-glycerol.

Although loss of *PEX11*α had no effect on PPARα-mediated peroxisome proliferation, *PEX11*α deficiency did lead to subtle changes of mitochondrial morphology in scattered hepatocytes of ciprofibrate-fed *PEX11*$\alpha^{-/-}$ animals (Fig. 7). A 2-week ciprofibrate diet led to proliferation of both mitochondria and peroxisomes in mouse hepatocytes. In *PEX11*$\alpha^{-/-}$ mouse livers, many mitochondria in midzonal and periportal hepatocytes contained unusual parallel cristae (Fig. 7D), and many mitochondria appeared to be tightly associated with lipid droplets (Fig. 7B). Ciprofibrate feeding also induced the association of mitochondria around lipid droplets in control animals (Fig. 7A), but the degree of mitochondrial ring formation was far lower than that in *PEX11*$\alpha^{-/-}$ animals. Moreover, mitochondria with parallel cristae were very rare in hepatocytes of control animals (Fig. 7C).

PEX11 is required for 4-PBA-mediated peroxisome proliferation. Ciprofibrate, WY-14,643, and DEHP act by stimulating the transcription factor PPARα/RxR (5, 32). Recent studies have shown that 4-PBA also induces the expression of *PEX11*α and peroxisome proliferation (28, 51). However, 4-PBA differs from previously described PPAs in that it acts independently of PPARα (G.-X. Dong and K. D. Smith, unpublished data) and can induce peroxisome proliferation in cultured human and mouse fibroblasts. When MEFs from control and *PEX11*$\alpha^{-/-}$ animals were examined for their response to 4-PBA, we found that the loss of *PEX11*α eliminated the peroxisome proliferation response to 4-PBA (Table 1).

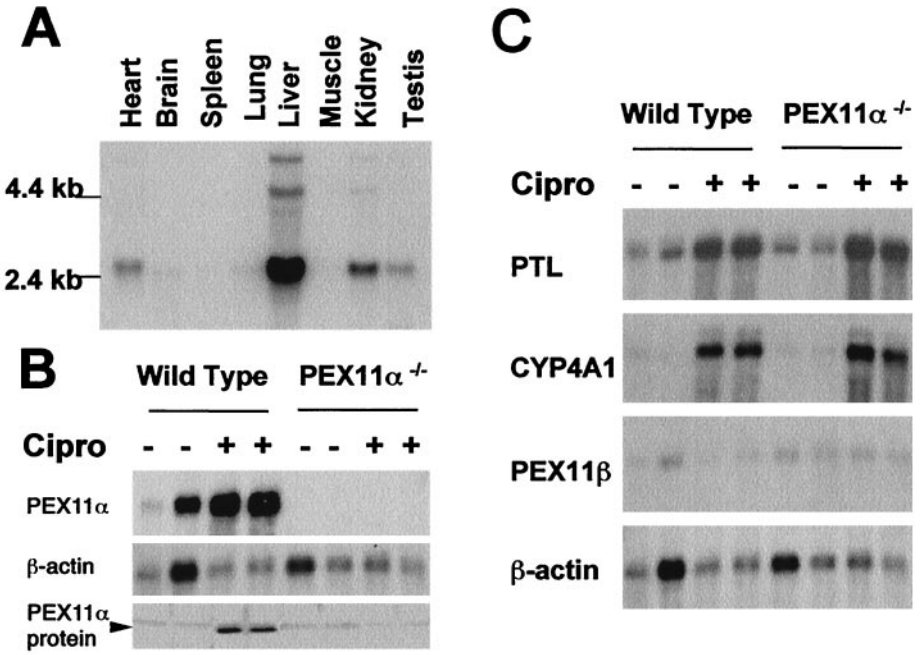

FIG. 5. PEX11α expression and role in PPA-mediated gene expression. (A) Abundance of *PEX11*α mRNA in mouse tissues. The mobilities of the 4.4- and 2.4-kb RNA standards are shown to the left of the blot. (B) *PEX11*α mRNA (top) and protein (bottom) are induced by ciprofibrate. The Northern blot was the same blot as in panel C. (C) Normal transcriptional responses of *PEX11*$\alpha^{-/-}$ mice to ciprofibrate. Total RNA was isolated from control and *PEX11*$\alpha^{-/-}$ mice fed either standard chow or chow supplemented with 0.0125% ciprofibrate for 2 weeks and then analyzed by Northern blotting with radioactively labeled *PTL*, *CYP4A1*, *PEX11*β, and β-actin cDNA probes as indicated.

Phenotypes of *PEX11*$\alpha^{-/-}$/*PEX11*$\beta^{-/-}$ mice. Mammals express both a *PEX11*α and a *PEX11*β gene (1, 2, 31, 38). We previously reported that loss of *PEX11*β reduces peroxisome abundance (though only about twofold), causes only a very mild defect in peroxisomal fatty acid β-oxidation (about 40%) and peroxisomal ether-lipid synthesis (about 20%), and has no effect on peroxisomal protein import (22). Nevertheless, *PEX11*$\beta^{-/-}$ mice display many of the pathological features of Zellweger syndrome, a disease that is typically associated with severe defects in peroxisomal protein import and virtually all peroxisomal metabolic functions (22). These pathologies include an intrauterine growth defect, severe hypotonia, and neonatal lethality. Histological examination of *PEX11*$\beta^{-/-}$ animals revealed additional similarities to Zellweger syndrome and Zellweger syndrome mice, including a neuronal migration defect, enhanced neuronal apoptosis, and a tissue-specific pattern of developmental delay (22).

To determine the effects of losing both the *PEX11*α and *PEX11*β genes, we generated doubly homozygous *PEX11*$\alpha^{-/-}$/*PEX11*$\beta^{-/-}$ mice by crossing mice that were both (i) heterozygous for the *PEX11*β lesion and (ii) either heterozygous or homozygous for the *PEX11*α lesion. Like *PEX11*$\beta^{-/-}$ mice, doubly homozygous *PEX11*$\alpha^{-/-}$/*PEX11*$\beta^{-/-}$ mice display an intrauterine growth defect, hypotonia, and neonatal or embryonic lethality (Table 2) but have only mild defects in peroxisomal metabolic functions (Fig. 8) and no defect in peroxisomal protein import (data not shown). As for peroxisome abundance, *PEX11*$\alpha^{-/-}$/*PEX11*$\beta^{-/-}$ cells had approximately half the numbers of peroxisomes of WT control animals and the same numbers of peroxisomes as did *PEX11*$\beta^{-/-}$ cells (Fig. 9A).

***PEX11*γ, a third *PEX11* gene of mammals.** At the outset of this study, we hypothesized that mammals expressed two PEX11 proteins and that peroxisome division requires at least one PEX11 protein (38). However, we recently identified a third mammalian gene, *PEX11*γ (Fig. 10A), which is expressed in both mice and humans (Fig. 10B). We performed a phylogenetic analysis of the known PEX11 proteins, which suggests that the *PEX11*γ gene defines a subfamily of PEX11 proteins that is distinct from the branch that includes the mammalian PEX11α and PEX11β proteins (Fig. 11). Northern analysis revealed that the expression of *PEX11*γ was tissue specific, with very high levels in liver but much lower levels in other tissues (Fig. 12A) and levels below the limit of detection in MEFs (data not shown). Additional experiments revealed that *PEX11*γ expression was not induced by ciprofibrate (Fig. 12B). Furthermore, no change in *PEX11*γ expression was detected in cells lacking either *PEX11*α or *PEX11*β (Fig. 12C).

To determine whether *PEX11*γ encoded a peroxisomal protein, we modified the *PEX11*γ cDNA so that it encoded a myc epitope tag at the either the 5′ or the 3′ end of the open reading frame. The corresponding cDNAs were placed in a mammalian cell expression vector, and the resulting plasmids (pcDNA3-myc*PEX11*γ and pcDNA3-*PEX11*γmyc) were transfected into the human fibroblast cell line 5756-TI. The cells were subsequently processed for immunofluorescence microscopy with antibodies to the myc epitope tag and to the peroxisomal marker protein PEX14 (Fig. 13). The colocalization of PEX11γ and PEX14 demonstrates that PEX11γ, like PEX11α and PEX11β, is a peroxisomal protein. Furthermore, the ability to detect the myc epitope tag at both the N and C termini of PEX11γ when only the plasma membrane is permeabilized

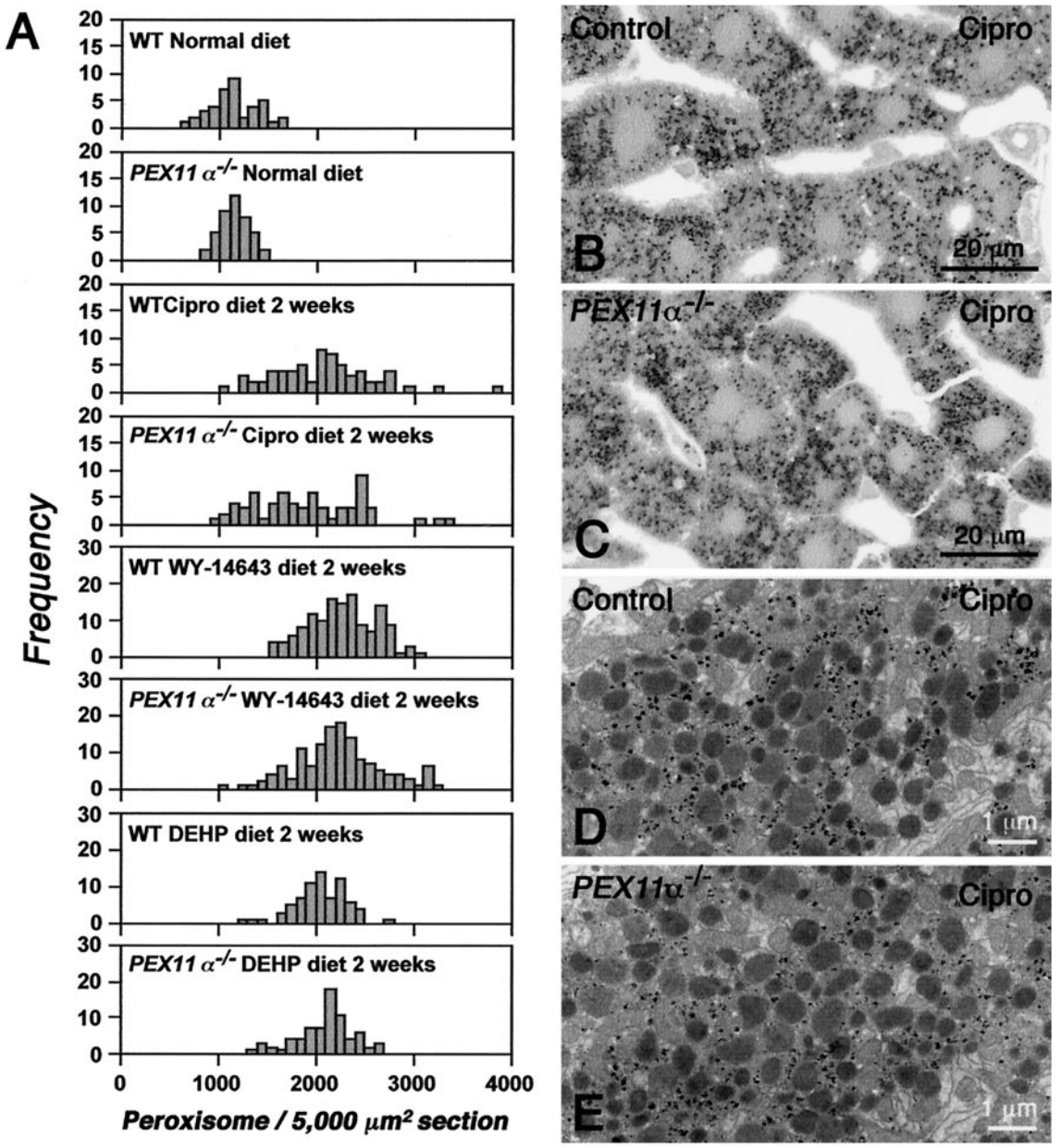

FIG. 6. Loss of *PEX11*α had no effect on PPA-mediated peroxisome proliferation. (A) Peroxisome abundance in the livers of control and *PEX11*$\alpha^{-/-}$ mice. Control and *PEX11*$\alpha^{-/-}$ mice were treated with ciprofibrate, WY-14,643, and DEHP as described in Materials and Methods for 2 weeks, and peroxisomes present in 50 to 80 fields surrounding the hepatic central veins in semithin liver sections were counted. Results here are presented as the peroxisome abundance distribution profile. Note that, after ciprofibrate, WY-14,643, and DEHP treatment, profile shifts in control and *PEX11*$\alpha^{-/-}$ mice were comparable. (B to E) Peroxisome distribution and morphology in ciprofibrate-fed control (B and D) and *PEX11*$\alpha^{-/-}$ (C and E) mice. Mice were fed with ciprofibrate as described in Materials and Methods for 2 weeks, fixed liver sections were stained with alkaline DAB and postfixed with reduced osmium, and then 0.5-μm semithin sections were analyzed under a light microscope (B and C) and ultrathin sections were analyzed under an electron microscope (D and E). All images are from hepatic central vein regions. There were no pronounced peroxisomal distribution and morphology differences between control and *PEX11*α-deficient mice.

and the peroxisomal membrane is intact suggests that PEX11γ is a peroxisomal membrane protein with both its N and C termini exposed to the cytoplasm. As for the consequences of *PEX11*γ overexpression, we did not observe any increase in peroxisome abundance. In fact, if overexpression of *PEX11*γmyc had any effect, it was to induce the tubulation, enlargement, and clustering of peroxisomes (Fig. 13C, D, G, and H).

DISCUSSION

Previous studies have implicated PEX11 proteins as effectors of peroxisome division (1, 2, 9, 23, 24, 27, 31, 36, 38) and established that *PEX11*α expression is induced by activation of PPARα (31, 38), which also induces peroxisome division (5, 32). These and other observations led us in a previous paper to propose that *PEX11*α plays an important role in the peroxi-

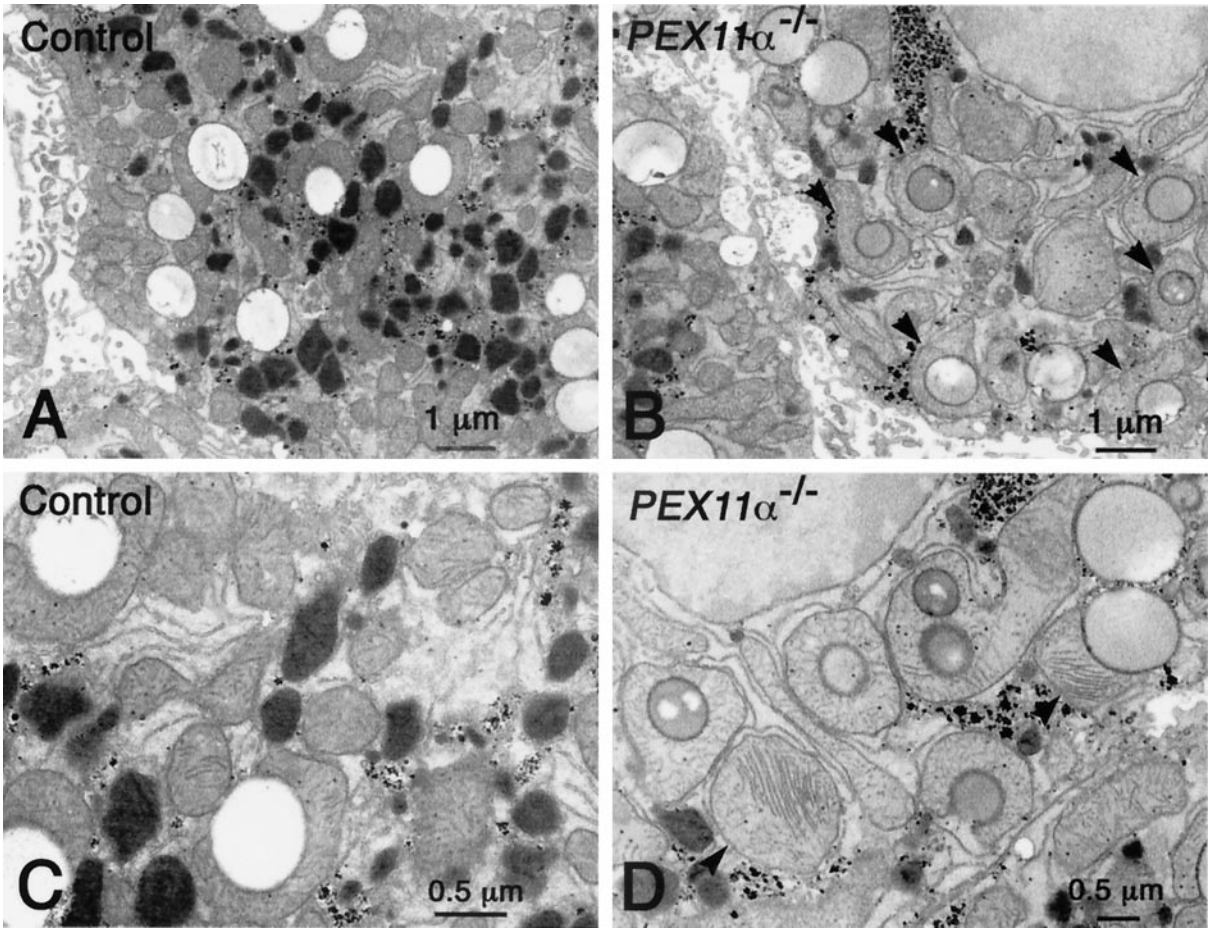

FIG. 7. Mitochondrial morphology defects in portal hepatocytes of ciprofibrate-fed *PEX11*$\alpha^{-/-}$ mice. Control (A and C) and *PEX11*$\alpha^{-/-}$ (B and D) mice were fed with ciprofibrate as described in Materials and Methods for 2 weeks, fixed liver sections were stained with alkaline DAB and postfixed with reduced osmium, and then ultrathin sections were analyzed under an electron microscope. All images were from the midzonal and periportal areas. In ciprofibrate-treated *PEX11*$\alpha^{-/-}$ mouse livers (B and D), many mitochondria contained unusual parallel cristae (arrowheads in panel D) and were tightly ringed around lipid droplets (arrowheads in panel B).

some proliferation response induced by activators of PPARα (38). Our analysis of *PEX11*$\alpha^{-/-}$ mice does not support this hypothesis but does show that *PEX11*α is required for peroxisome proliferation in response to 4-PBA, a drug that acts independently of PPARα.

PEX11$\alpha^{-/-}$ mice had no change in peroxisome abundance when fed a normal diet. In addition, each of three PPARα activators (ciprofibrate, WY-14,643, and DEHP) induced a normal peroxisome proliferation response in *PEX11*$\alpha^{-/-}$ mice. The simplest explanation for this result is that *PEX11*α is not involved in this process. However, it is possible that cells compensate for the loss of *PEX11*α by increasing PEX11β and/or PEX11γ activity. This does not appear to be likely, because *PEX11*β and *PEX11*γ mRNA levels were not elevated in *PEX11*$\alpha^{-/-}$ mice, but the effect could be mediated at some point other than mRNA abundance.

If PEX11α is not involved in the pathway of PPARα activation-mediated peroxisome proliferation, what are some other possible mechanisms that could link PPARα activation to peroxisome proliferation? One possibility is that it involves a nontranscriptional activation of PEX11β and/or PEX11γ activity.

TABLE 1. Effect of 4-PBA on peroxisome proliferation in PEX11α-knockout (KO) MEFs[a]

Cell line	No. of peroxisomes/cell		Increase (fold)
	Untreated	4-PBA treated	
WT-22	297 ± 53	466 ± 164	
WT-74	289 ± 113	457 ± 58	
WT-68	318 ± 70	464 ± 89	
WT-78	311 ± 37	449 ± 72	
WT-82	321 ± 42	513 ± 85	
Mean ± SD	307 ± 63	470 ± 94	1.53
PEX11α KO-26	298 ± 90	291 ± 56	
PEX11α KO-30	300 ± 47	317 ± 41	
PEX11α KO-85	349 ± 48	356 ± 45	
PEX11α KO-87	355 ± 73	353 ± 69	
PEX11α KO-89	351 ± 47	345 ± 39	
Mean ± SD	331 ± 61	332 ± 50	1.00

[a] Control and *PEX11*$\alpha^{-/-}$ MEFs were cultured in standard medium supplemented with 5 mM 4-PBA for 10 days, fixed, and processed for indirect immunofluorescence for catalase and PEX14. Cell images were then taken under a normal immunofluorescence microscope, and the peroxisomes in each of 12 cells were counted by hand.

TABLE 2. Survival rates and sizes of newborn mice with different genotypes at the *PEX11*α and *PEX11*β loci

Mouse genotype	Survival rate (%)	Size (g)
PEX11$\alpha^{+/+}/\beta^{+/+}$	100	1.39 ± 0.09
PEX11$\alpha^{-/-}/\beta^{+/+}$	100	1.38 ± 0.09
PEX11$\alpha^{+/+}/\beta^{-/-}$	0	0.84 ± 0.09
PEX11$\alpha^{-/-}/\beta^{-/-}$	0 (0/7)[a]	0.81 ± 0.11

[a] Two additional *PEX11*$\alpha^{-/-}/\beta^{-/-}$ mice die before birth.

Another is that it involves the activation of DLP1 (15, 16), a GTPase required for peroxisome division in mammalian cells (Li and Gould, submitted). However, it is known that peroxisome abundance is under metabolic control (7) and that activation of PPARα affects numerous metabolic pathways (32), raising the possibility that this peroxisome proliferation pathway is mediated through some type of metabolic control (7).

Although *PEX11*α is not required for peroxisome proliferation in response to PPARα activation, it is required for peroxisome proliferation in response to 4-PBA. 4-PBA induces peroxisome abundance approximately twofold in both human and mouse fibroblast cells, induces a similar increase in the abundance of *PEX11*α mRNA, and elevates the peroxisomal fatty acid β-oxidation activity (28, 51). A recent study has established that 4-PBA-mediated peroxisome proliferation is unaffected in MEFs from mice lacking the PPARα-encoding gene (Dong and Smith, unpublished), indicating that the mechanism of peroxisome proliferation in response to 4-PBA is distinct from that used by activators of PPARα. Here we find some support for this hypothesis by showing that *PEX11*α is required for the peroxisome proliferation response to 4-PBA. 4-PBA might raise peroxisome abundance solely by its effects on *PEX11*α expression, but this conclusion is preliminary, given that 4-PBA alters the transcriptional profile of many genes and affects many processes (8, 17).

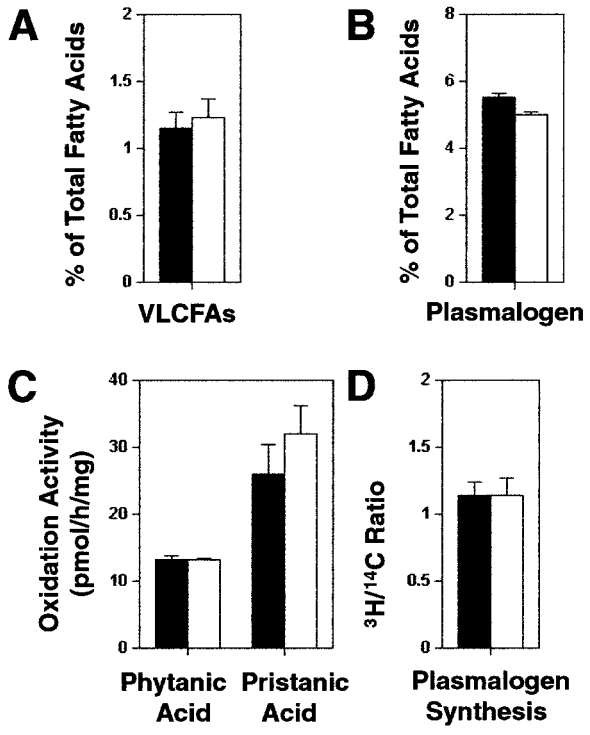

FIG. 8. Biochemical properties of *PEX11*$\alpha^{-/-}$/*PEX11*$\beta^{-/-}$ cells. In all graphs, the solid bar represents the average value obtained with control samples, the open bar represents the average value obtained with *PEX11*$\alpha^{-/-}$/*PEX11*$\beta^{-/-}$ samples, and the brackets represent 1 standard deviation. (A) VLCFA levels in MEFs of the control and *PEX11*$\alpha^{-/-}$/*PEX11*$\beta^{-/-}$ mice, expressed as a percentage of total fatty acids. (B) Plasmalogen levels in cultured MEFs, expressed as a percentage of total fatty acids. (C) Peroxisomal branched-chain fatty acid α- and β-oxidation activities in cultured MEFs. (D) Plasmalogen synthesis activities in cultured MEFs expressed as a ratio of the peroxisomal incorporation of [^{14}C]hexadecanol and the microsomal incorporation of the [^{3}H]hexadecyl-glycerol.

In addition to assessing peroxisome abundance and PPA-mediated peroxisome proliferation, we also tested whether the loss of PEX11α had any discernible effect on peroxisomal metabolic activities. The three most important peroxisomal metabolic functions are the β-oxidation of fatty acids, the α-oxidation of fatty acids, and the synthesis of ether-linked lipids (46, 48). The loss of *PEX11*α had no effect on these pathways. The relatively benign nature of *PEX11*α deficiency stands in sharp contrast to the severe consequences of *PEX11*β deficiency, which causes a significant reduction in peroxisome abundance and a series of pathologies similar to those of Zellweger syndrome (22).

The identification of a role for *PEX11*α in the response to 4-PBA, as well as our observation that it is not required for the response to more classical PPAs, broadens our understanding of this gene but does not provide a comprehensive understanding of its physiological roles. Likewise, our understanding of how PEX11 proteins participate in peroxisome division is only partly enlightened by the present study. However, it is useful to compare the process of peroxisome division to paradigms of vesicle budding in other organelle systems (21). Studies of COPII-mediated budding from the endoplasmic reticulum, COPI-mediated budding from the Golgi complex, and clathin-mediated budding from the trans-Golgi network and plasma membrane suggest that there are two general classes of organelle division factors. One class includes the proteins that are essential for division and directly execute the vesicle budding event, while the other class represents the recruitment factors that help bring the division machinery to the organelle membrane. In the case of peroxisomes, two sets of proteins have been implicated in peroxisome division: the PEX11 proteins and the VPS1/DLP1 GTPases. These differ considerably in their properties. The loss of the VPS1/DLP1 GTPases appears to block peroxisome division completely, but their overexpression has no stimulatory effect on division (13; Li and Gould, submitted). In contrast, loss of any or all PEX11 proteins has a less severe effect on peroxisome abundance but PEX11 overexpression strongly promotes peroxisome division (23; Li and Gould, submitted). Based on these limited results, one might predict that the VPS1/DLP1 GTPases are components of the peroxisome division machinery whereas PEX11 proteins might act by recruiting this and other components of the putative peroxisome division machinery to the organelle. This model is only valid if there are multiple recruitment mechanisms. These clearly exist for other organelle division processes (21), and the presence of multiple *PEX11* genes in

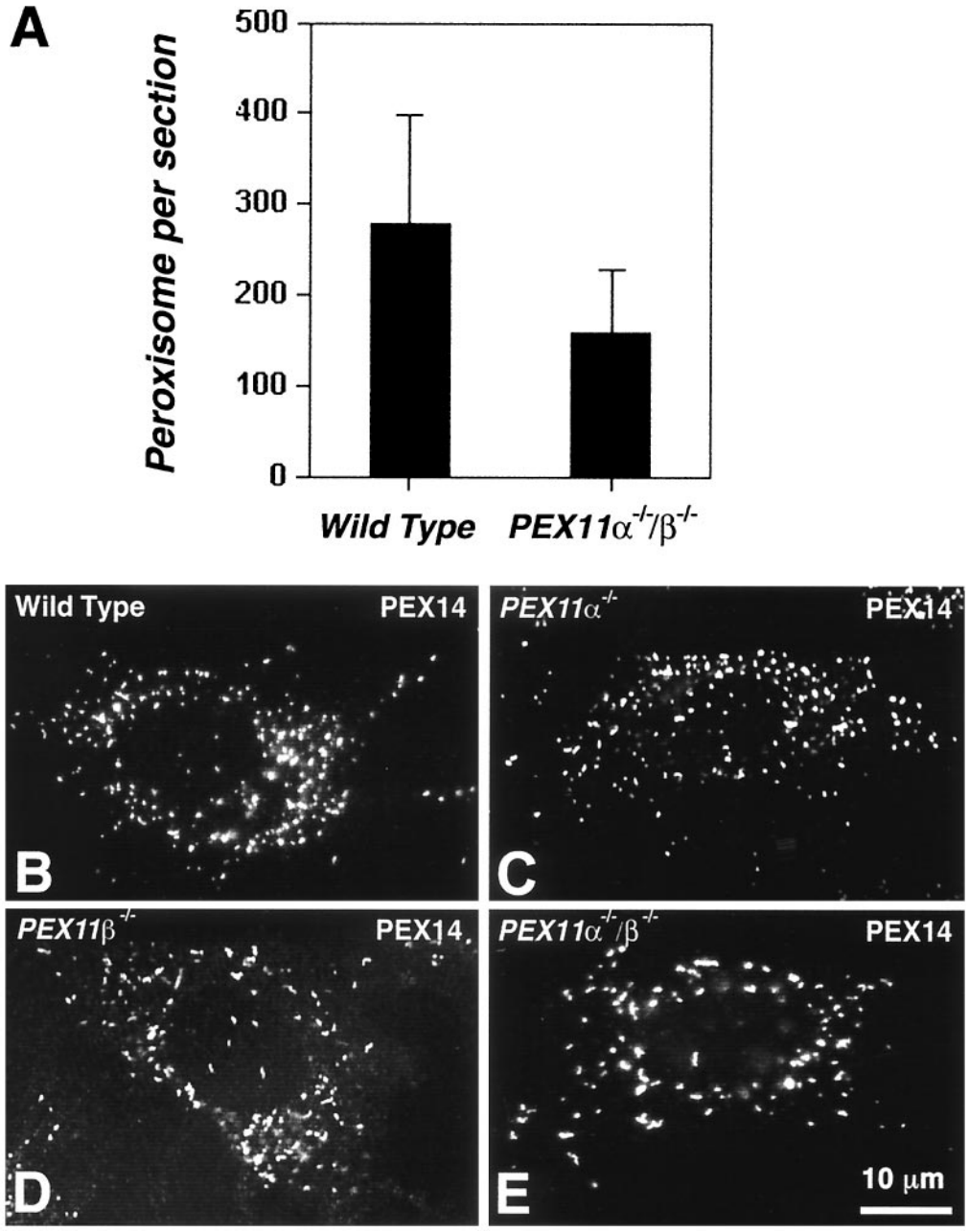

FIG. 9. Peroxisome abundance in *PEX11*$\alpha^{-/-}$/*PEX11*$\beta^{-/-}$ cells. MEFs from control and *PEX11*$\alpha^{-/-}$/*PEX11*$\beta^{-/-}$ animals were fixed, permeabilized with 1% Triton X-100, and processed for indirect immunofluorescence with antibodies to PEX14, a peroxisomal integral membrane protein. Peroxisomes present in at least 100 randomly selected fibroblasts from four cell lines were counted for each group. Results in panel A are presented as the average peroxisome abundances ± 1 standard deviation. Representative images are shown for WT control cells (B), *PEX11*$\alpha^{-/-}$ cells (C), *PEX11*$\beta^{-/-}$ cells (D), and *PEX11*$\alpha^{-/-}$/*PEX11*$\beta^{-/-}$ cells (E).

mammals also lends support to this notion. Our results add a small level of support to this model of peroxisome division by showing that PEX11 is required for the peroxisome proliferation response to 4-PBA. However, a direct test of this model remains to be performed.

At the outset of this study we hoped that we could eliminate PEX11 proteins from mice by disrupting the *PEX11*α and *PEX11*β genes. Our identification of a third *PEX11* gene, *PEX11*γ, makes it clear that we are still far from generating mice and murine cell lines that lack all PEX11 proteins. However, *PEX11*γ differs from *PEX11*α and *PEX11*β in that its overexpression does not induce peroxisome proliferation, its expression is not detectable in fibroblasts, and its expression is altered neither by classical PPAs nor by the loss of *PEX11*α or *PEX11*β. Thus, it may be that the phenotypes of *PEX11*$\alpha^{-/-}$/*PEX11*$\beta^{-/-}$ fibroblasts are the same as those that we will see for *PEX11*$\alpha^{-/-}$/*PEX11*$\beta^{-/-}$/*PEX11*$\gamma^{-/-}$ fibroblasts.

The hypothesis that PEX11 proteins act to recruit peroxi-

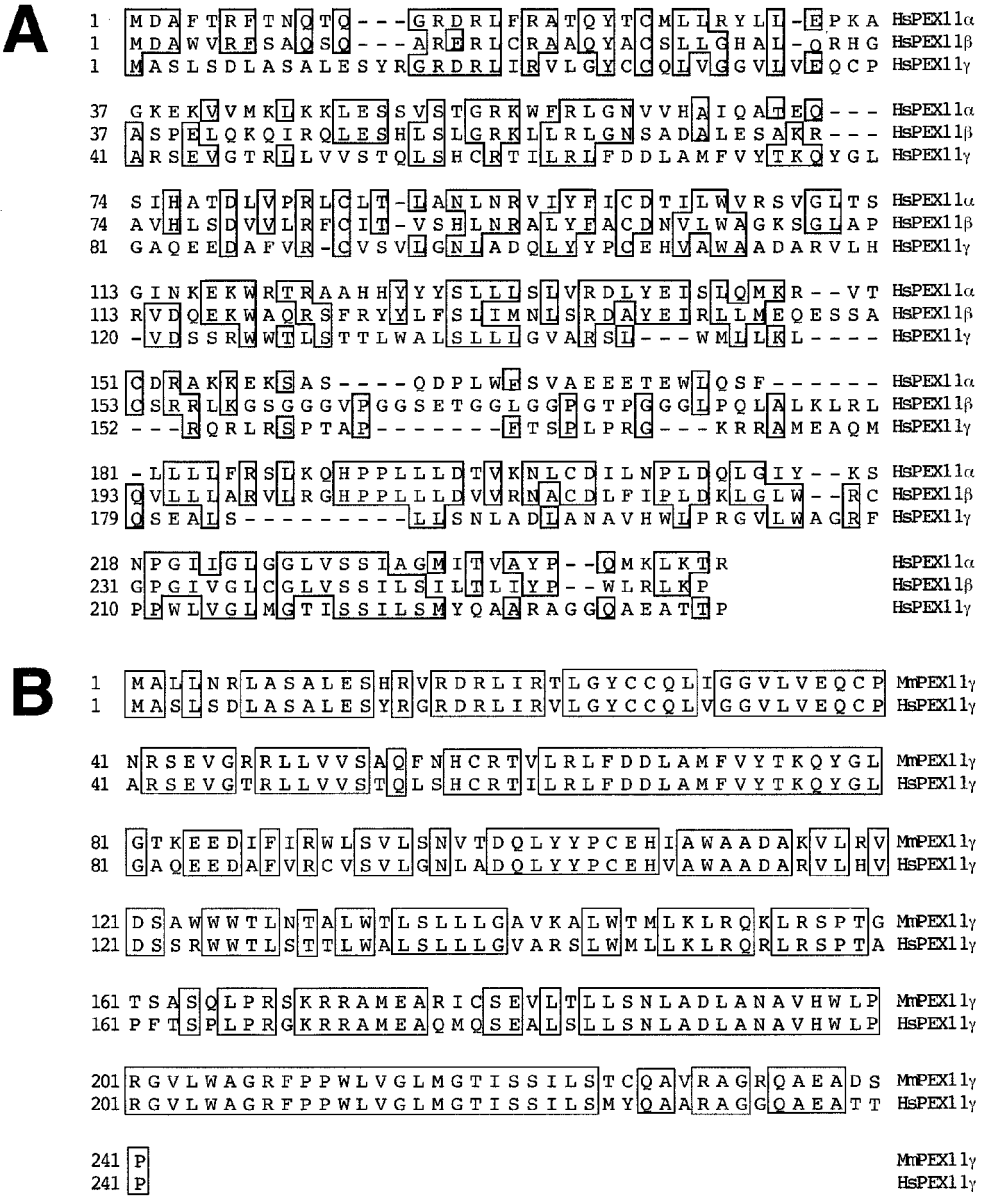

FIG. 10. Amino acid sequence analysis of mammalian PEX11γ. (A) Amino acid sequence alignment of human PEX11α, PEX11β, and PEX11γ. Sequences were aligned by the CLUSTAL method. Boxes represent amino acids present in at least two of the three proteins. (B) Amino acid sequence alignment of human and mouse PEX11γ proteins. Sequences were aligned by the CLUSTAL method, and boxes represent amino acids shared by these proteins.

some division factors is not new. Its original form, proposed by Passreiter et al. (31), was based on their report that rat PEX11α recruited the COPI vesicle coat to peroxisome membranes and that increased levels of PEX11α caused an increased rate of COPI-dependent vesicle budding from peroxisomes (31). In support of this hypothesis are the observations that the COPI-binding motif, KXKXX, is a conserved feature of mammalian PEX11α proteins, is present in PEX11 proteins from some lower eukaryotes (24, 38), and binds COPI in vitro (31) and that overexpression of PEX11α is sufficient to promote peroxisome division (31, 38). Against this hypothesis are the facts that many PEX11 proteins do not contain a COPI recruitment motif (35), that disruption of the KXKXX motif at the C terminus of PEX11 proteins has little or no effect on their ability to induce peroxisome proliferation (26, 38), and that brefeldin A, which disrupts COPI-mediated vesicle transport, has no effect on peroxisome biogenesis (40, 41, 44). Our results add the fact that loss of PEX11α has no effect on PPARα-mediated peroxisome proliferation. While it is not possible to conclude that COPI plays no role in peroxisome division, we can conclude that it plays at best an ancillary role in mammalian cells. However, we may find that peroxisome division is promoted by many factors, all of which are important but only a few of which are essential.

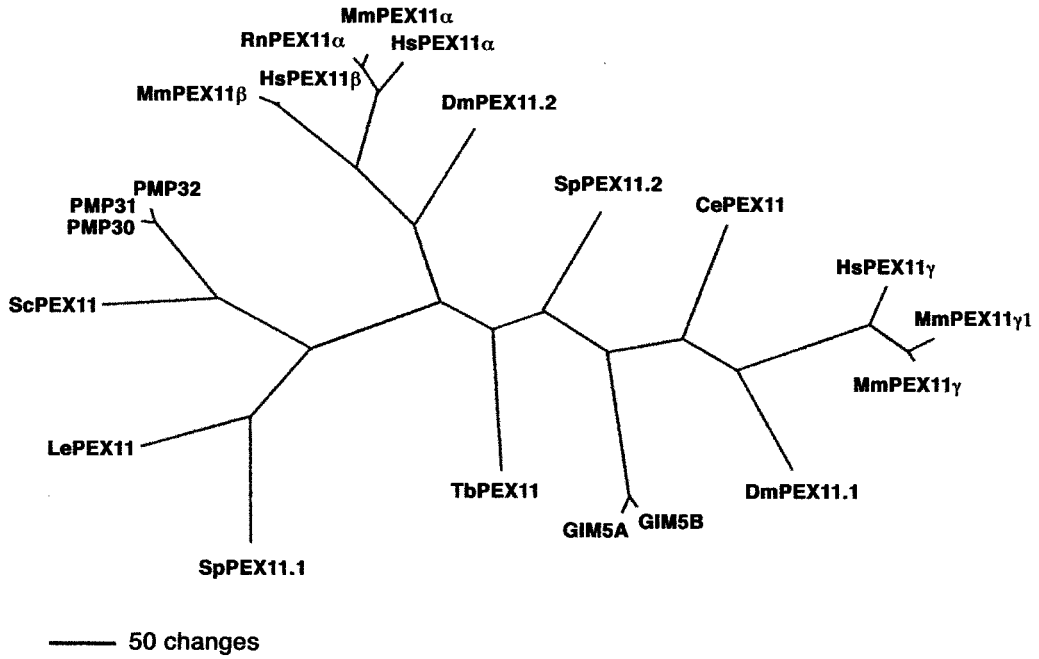

FIG. 11. Phylogram representation of amino acid sequence similarities among yeast and animal PEX11 proteins. Sequences are aligned by the Clustal W method, and an unrooted phylogram tree was generated with the PAUP program. These are based on the published sequences of human and mouse PEX11 proteins (38); rat PEX11α (31); *Trypanosoma brucei* TbPEX11 (24) and TbGIM5 (25) proteins; *Saccharomyces cerevisiae* ScPEX11 (9); and *Candida boidinii* PMP30, PMP31, and PMP32 proteins (36), as well as the database sequences for human and mouse PEX11γ proteins, a splicing isoform of mouse PEX11γ protein MmPEX11γ1 (GenBank accession no. BAB25302), *Lycopersicon esculentum* LePEX11 (AAF75750), *Caenorhabditis elegans* CePEX11 (CAB16857), *Drosophila melanogaster* DmPEX11.1 (AAF56119) and DmPEX11.2 (AAF58084), and *Schizosaccharomyces pombe* SpPEX11.1 (CAA93785 and CAB46672) and SpPEX11.2 (CAA93808).

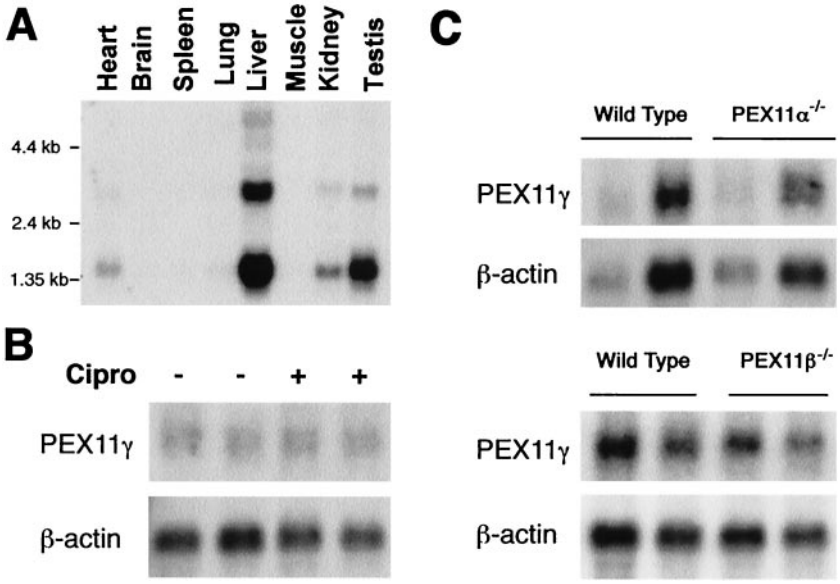

FIG. 12. Northern analysis of *PEX11*γ expression. (A) Abundance of *PEX11*γ mRNA in mouse tissues. A multitissue Northern blot filter was hybridized to a radiolabeled *PEX11*γ-specific cDNA probe and exposed to X-ray film. (B) Total liver RNA from mice fed normal rodent chow (lanes 1 and 2) and mice fed for 2 weeks with ciprofibrate-supplemented normal chow (lanes 3 and 4) were separated by denaturing agarose gel electrophoresis, transferred to a membrane, hybridized to a radiolabeled *PEX11*γ-specific cDNA probe, and exposed to X-ray film. (C) Total liver RNAs from control mice, *PEX11*$\alpha^{-/-}$ mice, and *PEX11*$\beta^{-/-}$ mice were separated by denaturing agarose gel electrophoresis, transferred to a membrane, hybridized to a radiolabeled *PEX11*γ-specific cDNA probe, and exposed to X-ray film.

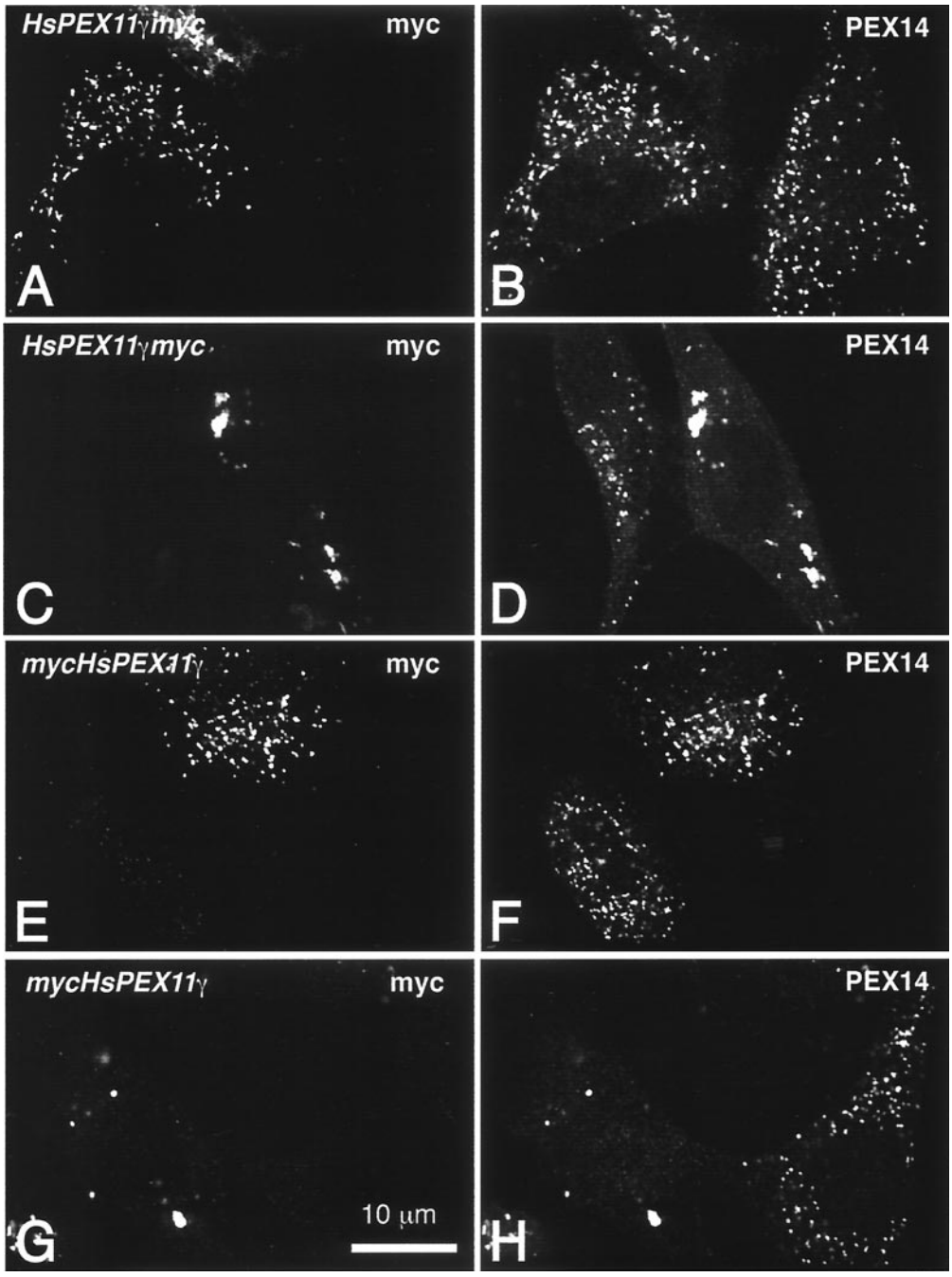

FIG. 13. PEX11γ encodes a peroxisomal membrane protein. Human skin fibroblast cells were transfected with pcDNA3-*HsPEX11*γmyc or pcDNA3-myc*HsPEX11*γ by electroporation. Two days after transfection the cells were processed for immunofluorescence microscopy with antibodies specific for the myc epitope tag (A, C, E, and G) and PEX14 (B, D, F, and H), a peroxisomal membrane protein. In these experiments, cells were fixed and then permeabilized with a limiting concentration of digitonin so that antibodies had access to cytoplasmically exposed epitopes but to not epitopes that resided within peroxisomes.

ACKNOWLEDGMENTS

We thank Ann and Hugo Moser for use of their laboratory for biochemical experiments and Stephanie Mihalik and Paul Watkins for help in determining α- and β-oxidation activities in fibroblasts and liver homogenates.

This work was supported by grants from the NIH to S.J.G. (DK59479 and HD10981) and D.V. (HD10981). D.V. is an investigator of the HHMI. E.B. was supported by a Max Kade Scholarship (Max Kade Foundation, New York, N.Y., and Deutsche Forschungsgemeinschaft, Germany).

REFERENCES

1. **Abe, I., and Y. Fujiki.** 1998. cDNA cloning and characterization of a constitutively expressed isoform of the human peroxin Pex11p. Biochem. Biophys. Res. Commun. **252:**529–533.
2. **Abe, I., K. Okumoto, S. Tamura, and Y. Fujiki.** 1998. Clofibrate-inducible,

28-kDa peroxisomal integral membrane protein is encoded by PEX11. FEBS Lett. **431:**468–472.
3. **Altschul, S. F., W. Gish, W. Miller, E. W. Myers, and D. J. Lipman.** 1990. Basic local alignment search tool. J. Mol. Biol. **215:**403–410.
4. **Bellu, A. R., M. Komori, I. J. van der Klei, J. A. Kiel, and M. Veenhuis.** 2001. Peroxisome biogenesis and selective degradation converge at Pex14p. J. Biol. Chem. **276:**44570–44574.
5. **Berger, J., and D. E. Moller.** 2002. The mechanisms of action of PPARs. Annu. Rev. Med. **53:**409–435.
6. **Chang, C. C., W. H. Lee, H. W. Moser, D. Valle, and S. J. Gould.** 1997. Isolation of the human PEX12 gene, mutated in group 3 of the peroxisome biogenesis disorders. Nat. Genet. **15:**385–388.
7. **Chang, C. C., S. South, D. Warren, J. Jones, A. B. Moser, H. W. Moser, and S. J. Gould.** 1999. Metabolic control of peroxisome abundance. J. Cell Sci. **112:**1579–1590.
8. **Chang, K. T., and K. T. Min.** 2002. Regulation of lifespan by histone deacetylase. Ageing Res. Rev. **1:**313–326.
9. **Erdmann, R., and G. Blobel.** 1995. Giant peroxisomes in oleic acid-induced *Saccharomyces cerevisiae* lacking the peroxisomal membrane protein Pmp27p. J. Cell Biol. **128:**509–523.
10. **Evan, G. E., G. K. Lewis, G. Ramsay, and J. M. Bishop.** 1985. Isolation of monoclonal antibodies specific for human c-myc proto-oncogene product. Mol. Cell. Biol. **5:**3610–3616.
11. **Fahimi, H. D.** 1969. Cytochemical localization of peroxidatic activity of catalase in rat hepatic microbodies (peroxisomes). J. Cell Biol. **43:**275–288.
12. **Gould, S. G., D. Valle, and G. V. Raymond.** 2001. The peroxisome biogenesis disorders, p. 3181–3217. *In* C. R. Scriver, A. L. Beaudet, W. S. Sly, and D. Valle (ed.), The metabolic and molecular bases of inherited disease, 8th ed., vol. 2. McGraw-Hill, New York, N.Y.
13. **Hoepfner, D., M. van den Berg, P. Philippsen, H. F. Tabak, and E. H. Hettema.** 2001. A role for Vps1p, actin, and the Myo2p motor in peroxisome abundance and inheritance in *Saccharomyces cerevisiae*. J. Cell Biol. **155:** 979–990.
14. **Hogan, B., R. Beddington, F. Costantini, and E. Lacy.** 1994. Manipulating the mouse embryo: a laboratory manual, 2nd ed. Cold Spring Harbor Laboratory Press, Cold Spring Harbor, N.Y.
15. **Imoto, M., I. Tachibana, and R. Urrutia.** 1998. Identification and functional characterization of a novel human protein highly related to the yeast dynamin-like GTPase Vps1p. J. Cell Sci. **111:**1341–1349.
16. **Kamimoto, T., Y. Nagai, H. Onogi, Y. Muro, T. Wakabayashi, and M. Hagiwara.** 1998. Dymple, a novel dynamin-like high molecular weight GTPase lacking a proline-rich carboxyl-terminal domain in mammalian cells. J. Biol. Chem. **273:**1044–1051.
17. **Kang, H. L., S. Benzer, and K. T. Min.** 2002. Life extension in Drosophila by feeding a drug. Proc. Natl. Acad. Sci. USA **99:**838–843.
18. **Karpichev, I. V., and G. M. Small.** 1998. Global regulatory functions of Oaf1p and Pip2p (Oaf2p), transcription factors that regulate genes encoding peroxisomal proteins in *Saccharomyces cerevisiae*. Mol. Cell. Biol. **18:**6560–6570.
19. **Kaufmann, W. E., C. Theda, S. Naidu, P. A. Watkins, A. B. Moser, and H. W. Moser.** 1996. Neuronal migration abnormality in peroxisomal bifunctional enzyme defect. Ann. Neurol. **39:**268–271.
20. **Kim, J., and D. J. Klionsky.** 2000. Autophagy, cytoplasm-to-vacuole targeting pathway, and pexophagy in yeast and mammalian cells. Annu. Rev. Biochem. **69:**303–342.
21. **Kirchhausen, T.** 2000. Three ways to make a vesicle. Nat. Rev. Mol. Cell Biol. **1:**187–198.
22. **Li, X., E. Baumgart, J. C. Morrell, G. Jimenez-Sanchez, D. Valle, and S. G. Gould.** 2002. PEX11β deficiency is lethal and impairs neuronal migration but does not abrogate peroxisome function. Mol. Cell. Biol. **22:**4358–4365.
23. **Li, X., and S. G. Gould.** 2002. PEX11 promotes peroxisome division independently of peroxisome metabolism. J. Cell Biol. **156:**643–651.
24. **Lorenz, P., A. G. Maier, E. Baumgart, R. Erdmann, and C. Clayton.** 1998. Elongation and clustering of glycosomes in *Trypanosoma brucei* overexpressing the glycosomal Pex11p. EMBO J. **17:**3542–3555.
25. **Maier, A., P. Lorenz, F. Voncken, and C. Clayton.** 2001. An essential dimeric membrane protein of trypanosome glycosomes. Mol. Microbiol. **39:**1443–1451.
26. **Maier, A. G., S. Schulreich, M. Bremser, and C. Clayton.** 2000. Binding of coatomer by the PEX11 C-terminus is not required for function. FEBS Lett. **484:**82–86.
27. **Marshall, P., Y. Krimkevich, R. Lark, J. Dyer, M. Veenhuis, and J. Goodman.** 1995. Pmp27 promotes peroxisomal proliferation. J. Cell Biol. **129:**345–355.
28. **McGuinness, M. C., H. P. Zhang, and K. D. Smith.** 2001. Evaluation of pharmacological induction of fatty acid beta-oxidation in X-linked adrenoleukodystrophy. Mol. Genet. Metab. **74:**256–263.
29. **Moser, A. B., N. Kreiter, L. Bezman, S. Lu, G. V. Raymond, S. Naidu, and H. W. Moser.** 1999. Plasma very long chain fatty acids in 3,000 peroxisome disease patients and 29,000 controls. Ann. Neurol. **45:**100–110.
30. **Moser, H. W.** 1999. Genotype-phenotype correlations in disorders of peroxisome biogenesis. Mol. Genet. Metab. **68:**316–327.
31. **Passreiter, M., M. Anton, D. Lay, R. Frank, C. Harter, F. T. Wieland, K. Gorgas, and W. W. Just.** 1998. Peroxisome biogenesis: involvement of ARF and coatomer. J. Cell Biol. **141:**373–383.
32. **Reddy, J. K., and T. Hashimoto.** 2001. Peroxisomal beta-oxidation and peroxisome proliferator-activated receptor alpha: an adaptive metabolic system. Annu. Rev. Nutr. **21:**193–230.
33. **Roscher, A., B. Molzer, H. Bernheimer, S. Stockler, I. Mutz, and F. Paltauf.** 1985. The cerebrohepatorenal (Zellweger) syndrome: an improved method for the biochemical diagnosis and its potential value for prenatal detection. Pediatr. Res. **19:**930–933.
34. **Rottensteiner, H., A. J. Kal, B. Hamilton, H. Ruis, and H. F. Tabak.** 1997. A heterodimer of the Zn2Cys6 transcription factors Pip2p and Oaf1p controls induction of genes encoding peroxisomal proteins in *Saccharomyces cerevisiae*. Eur. J. Biochem. **247:**776–783.
35. **Sacksteder, K. A., and S. J. Gould.** 2000. The genetics of peroxisome biogenesis. Annu. Rev. Genet. **34:**623–652.
36. **Sakai, Y., P. A. Marshall, A. Saiganji, K. Takabe, H. Saiki, N. Kato, and J. M. Goodman.** 1995. The *Candida boidinii* peroxisomal membrane protein Pmp30 has a role in peroxisomal proliferation and is functionally homologous to Pmp27 from *Saccharomyces cerevisiae*. J. Bacteriol. **177:**6773–6781.
37. **Sambrook, J., E. F. Fritsch, and T. Maniatis.** 1989. Molecular cloning: a laboratory manual, 2nd ed. Cold Spring Harbor Laboratory Press, Cold Spring Harbor, N.Y.
38. **Schrader, M., B. E. Reuber, J. C. Morrell, G. Jimenez-Sanchez, C. Obie, T. Stroh, D. Valle, T. A. Schroer, and S. J. Gould.** 1998. Expression of *PEX11*β mediates peroxisome proliferation in the absence of extracellular stimuli. J. Biol. Chem. **273:**29607–29614.
39. **Slawecki, M., G. Dodt, S. Steinberg, A. B. Moser, H. W. Moser, and S. J. Gould.** 1995. Identification of three distinct peroxisomal protein import defects in patients with peroxisomal biogenesis disorders. J. Cell Sci. **108:** 1817–1829.
40. **South, S. T., and S. J. Gould.** 1999. Peroxisome synthesis in the absence of pre-existing peroxisomes. J. Cell Biol. **144:**255–266.
41. **South, S. T., K. A. Sacksteder, X. Li, Y. Liu, and S. J. Gould.** 2000. Inhibitors of COPI and COPII do not block PEX3-mediated peroxisome synthesis. J. Cell Biol. **149:**1345–1360.
42. **Subramani, S.** 1998. Components involved in peroxisome import, biogenesis, proliferation, turnover, and movement. Physiol. Rev. **78:**171–188.
43. **van Roermund, C. W., H. F. Tabak, M. van Den Berg, R. J. Wanders, and E. H. Hettema.** 2000. Pex11p plays a primary role in medium-chain fatty acid oxidation, a process that affects peroxisome number and size in *Saccharomyces cerevisiae*. J. Cell Biol. **150:**489–498.
44. **Voorn-Brouwer, T., A. Kragt, H. F. Tabak, and B. Distel.** 2001. Peroxisomal membrane proteins are properly targeted to peroxisomes in the absence of COPI- and COPII-mediated vesicular transport. J. Cell Sci. **114:**2199–2204.
45. **Wanders, R. J., and J. M. Tager.** 1998. Lipid metabolism in peroxisomes in relation to human disease. Mol. Aspects Med. **19:**69–154.
46. **Wanders, R. J., P. Vreken, S. Ferdinandusse, G. A. Jansen, H. R. Waterham, C. W. van Roermund, and E. G. Van Grunsven.** 2001. Peroxisomal fatty acid alpha- and beta-oxidation in humans: enzymology, peroxisomal metabolite transporters and peroxisomal diseases. Biochem. Soc. Trans. **29:**250–267.
47. **Wanders, R. J. A., P. G. Barth, and H. S. A. Heymans.** 2001. Single peroxisomal enzyme deficiencies, p. 3219–3256. *In* C. R. Scriver, A. L. Beaudet, W. S. Sly, and D. Valle (ed.), The metabolic and molecular bases of inherited disease, 8th ed., vol. 2. McGraw-Hill, New York, N.Y.
48. **Wanders, R. J. A., C. Jakobs, and O. H. Skejldal.** 2001. Refsum disease, p. 3303–3322. *In* C. R. Scriver, A. L. Beaudet, W. S. Sly, and D. Valle (ed.), The metabolic and molecular bases of inherited disease, 8th ed., vol. 2. McGraw-Hill, New York, N.Y.
49. **Wang, T., A. M. Lawler, G. Steel, and D. Valle.** 1995. Paradoxical hypoornithenemia and neonatal lethality in mice with targeted disruption of the OAT gene. Nat. Genet. **11:**185–190.
50. **Watkins, P., E. J. Ferrell, J. Pedersen, and G. Hoefler.** 1991. Peroxisomal fatty acid β-oxidation in HepG2 cells. Arch. Biochem. Biophys. **289:**329–366.
51. **Wei, H., S. Kemp, M. C. McGuinness, A. B. Moser, and K. D. Smith.** 2000. Pharmacological induction of peroxisomes in peroxisome biogenesis disorders. Ann. Neurol. **47:**286–296.
52. **Yahraus, T., N. Braverman, G. Dodt, J. E. Kalish, J. C. Morrell, H. W. Moser, D. Valle, and S. J. Gould.** 1996. The peroxisome biogenesis disorder group 4 gene, *PXAAA1*, encodes a cytoplasmic ATPase required for stability of the PTS1 receptor. EMBO J. **15:**2914–2923.
53. **Zenger-Hain, J., D. A. Craft, and W. B. Rizzo.** 1992. Diagnosis of inborn errors of phytanic acid oxidation using tritiated phytanic acid. Prog. Clin. Biol. Res. **375:**399–407.